Three dimensional transition solid elements for mesh gradation

*Syeda Ammara Shabbir[1], Shahzadi Shamaila[2], Rehana Sharif[3], Saira Riaz[4] and Shahzad Naseem[5]

[1), 2),3)] *Department of Physics, University of Engineering and Technology, Lahore, Pakistan*
[4),5)] *Centre for Solid State Physics, University of the Punjab, Lahore*

ABSTRACT

The Multiwalled carbon nanotubes (MWCNTs) thin film based electrode was fabricated by electrophoretic deposition and modified with Nickel (Ni) Nanoparticles to fabricate Ni/CNTs nanocomposite sensor for nonenzymatic glucose detection. The expensive glassy carbon (GC) electrode is replaced by Fluorine doped tin oxide (FTO) glass containing CNTs film to confine the Ni nanoparticles growth by electrodeposition through Cyclic Voltammetry (CV). The UV-VIS and XRD analysis revealed the successful deposition of Ni nanoparticles on the CNTs modified electrode. The Scanning electron microscope (SEM) confirmed the surface morphology of electrodeposited Ni on CNT film as uniformly dispersed particles. The electrocatalytic activity of electrode to the glucose oxidation was investigated in alkaline medium by Cyclic Voltammetry (CV) and amperometric measurements. The fabricated sensor exhibited a fast response time of less than 4s and the sensitivity 605.0 μA mM^{-1}cm^{-2} with linear concentration range (0.005–3.0 mM) having detection limit 5.0 μM. Due to simple preparation of sensor, Ni-CNTs nanocomposite electrodes are a suitable candidate for reliable determination of glucose with good stability.

Key words: Electrophoretic deposition (EPD), Fluorine doped tin oxide (FTO) substrate, Carbon Nanotubes, Copper Nanoparticles, Non enzymatic electrocatalysis, Glucose sensor.

1. Introduction

Diabetes mellitus being an extremely extensive disease, transporting metabolic disorders and affecting about 220 million people around the world. The mortality and morbidity caused by hyperglycemia and insulin deficiency is imitated by higher or lower concentration of blood glucose as compared to the normal range (4.5 – 6.5 mM) [1]. Therefore to establish a simple and rapid glucose sensing system is of significant

---

[1] Corresponding Author

importance having high stability, sensitivity and selectivity to distinguish different levels of glucose. [2-4].The electrochemical glucose sensors, widely used till today, are enzymatic with high sensitivity and good reliability. However, the catalytic response of the enzyme glucose oxidase (GOx) is sensitive to chemical reagents, pH, temperature and humidity, causing the instability and enzyme damage. Therefore, highly selective nonenzymatic glucose sensors, based on direct glucose oxidation on the surface of electrode without using enzyme are desired. The non-enzymatic biosensors [5, 6] have attractive benefits of simple and inexpensive fabrication with good reproducibility and high stability. Most of these non-enzymatic glucose sensors are amperometric.

The Electrode material with highly active surface area plays an important role in the glucose electroxidation. Therefore, nanomaterials such as transition metallic nanoparticles and Carbon nanotubes (CNTs) have been utilized extensively in biosensors. CNTs are of great importance because of its high chemical stability [7-10] and remarkable physical and electrical properties. Transition metallic nanoparticles (NPs) increase the electrochemical activities due to high surface area, enhanced catalysis and good biocompatibility. [10-12]. Hence it is a significant approach to use them for nonenzymatic glucose sensors , such as Pt NPs [13,14], Cu NPs [15,16], Au NPs [17,18], Ni NPs [19], CNTs modified electrodes [20,21] and Cu NPs with CNTs [22,23] . The fast amperometric glucose detection and high sensitivity have been reported owing to increase in electroactive surface area. This provides the more electron transfer during oxidation reactions of glucose. The electrode materials for glucose analysis based on Nickel NPs are of primary interest for its better catalytic activity, detection limit, range of response and mainly stability [24]. It has been revealed that the catalyst properties can be improved by varying the surface profile, grain size and texture. Therefore it is a critical requirement to produce nanosized catalysts with improved activities [25]. Continuous efforts have been made to fabricate effectively dispersed Ni/CNTs composites with increased catalytic activity; however, during recent years few reports developed the nonenzymatic glucose sensor with the highly dispersed Ni/CNTs nanocomposites electrodes.

In this work a new, inexpensive and facile route have been employed for the Ni/CNTs composite fabrication for the nonenzymatic sensing of glucose and it delivered fairly high sensitivity, good selectivity and reproducibility and fast current response .In fact, the fabrication of pure Ni Nanoparticles is difficult, as they provide poor stability during electroanalysis and easily oxidized in air [12]. In this project, Ni nanoclusters were electrodeposited by Cyclic voltammetry on CNTs modified electrode fabricated by electrophoretic deposition. COOH functionalized CNTs were treated with SDS (Sodium dodecyl sulphate) to get the most stable suspension for CNTs electrode fabrication through Electrophoretic deposition (EPD). The rigid control of deposition rate and film thickness during EPD provides an excellent film uniformity and strong adhesion on electrode surface which is not possible in drop casting and other wet chemical techniques for thin films fabrication [26–28]. This fabricated Ni/CNTs composite provides more uniform copper deposition on CNTs electrode with better sensing parameters as compared to previously published works with other techniques.

2. EXPERIMENTAL DETAILS

2.1 Reagents and materials

MWCNTs (diameter~10–20 nm, length~10 –30 μm, Purity >95%) were purchased from Jinzhou Hancheng Import & Export Co., Ltd. in China and used as received. The chemicals, Sodium dodecyl sulphate (SDS), Boric acid (H_3BO_3), Nickel sulphate ($NiSO_4.6H_2O$), Nickel Chloride ($NiCl_2.6H_2O$), Sodium hydroxide (NaOH), Potassium Ferricyanide (K_3 [$Fe(CN)_6$]) and reagents Nitric acid (HNO_3) and Sulphuric acid (H_2SO_4)were purchased from Merck India. Deionized (DI) water was utilized throughout the experiment for aqueous solutions.

2.2 Preparation of Ni/CNTs/FTO nanocomposite electrode.

The CNTs were carboxylic acid (COOH) functionalized through sonication at $60°C$ for 6 hours in HNO_3/ $H2SO_4$ (1:3, 50 ml) mixture. The acid mixture was then re-suspended in DI water following centrifugation at 8,500 rpm for 30 min. The repetitive centrifugation was performed to achieve the neutral pH solution. The residue was then dried at $25°C$ for 24 h to yield the COOH- functionalized MWNTs (f-CNTs). To get the effective stable suspension for EPD, f-CNTs were dissolved in aqueous micellar solutions of the anionic surfactant Sodium dodecyl sulphate (SDS). EPD was conducted using a DC power supply by applying optimized DC voltage (35 V/cm) for 3 min deposition time at room temperature. The working electrode was FTO substrate and the graphite used as counter electrode. Both electrodes in the EPD cell were fixed parallel to each other. DC voltage was applied at a constant distance between electrodes. The CNTs coated FTO substrate was cleaned with DI water to remove any contaminants and dried at room temperature. The obtained electrode was arranged for electrodeposition of copper. The Nickel (Ni) electrodeposition was carried out in Boric acid solution of Nickel sulphate ($Ni_2So_4.6H_2O$) and Nickel Chloride ($NiCl_2.6H_2O$) by cyclic voltammetry. The scan rate was 100 mV/s and performed in the potential window of 0.5 to 1.1 V. The cyclic number was kept 30 to achieve the high reproducibility and sensitivity of the electrodes. The fabricated Ni/CNTs composite electrode was stored at room temperature.

2.3 Characterization Techniques:

The CNTs and Ni/CNTs composite electrode was characterized by 2001 Bruker AXS diffractometer using CuKα radiation. The absorption spectrum of both electrodes was recorded using UV-VIS spectrophotometer. The surface morphology of the modified electrodes was characterized by scanning electron microscopy (SEM; JSM-6480LV). To study the electrochemical properties of the modified electrode cyclic voltammetry was conducted using the Princeton 263A electrochemical work station having three electrode configurations with graphite as a counter electrode, a saturated calomel reference electrode, and CNT film electrode as working electrode.
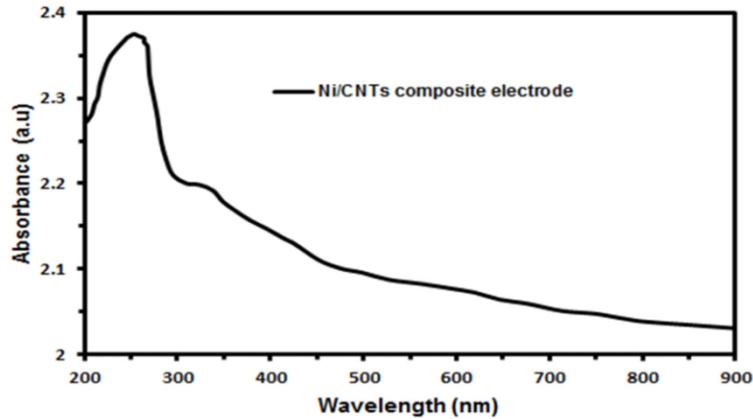
Figure 1: UV-VIS spectrograph of Ni/CNTs/FTO nanocomposite Electrode

3. Results and Discussions

3.1 Characterization of Ni/CNTs/FTO nanocomposite electrode
This work provides a simple and inexpensive fabrication approach of Ni/CNTs nanocomposite. The use of electrophoreticaly deposited CNTs electrode has advantages of excellent film uniformity and strong adhesion.

The optical absorbance of electrodeposited Ni film on electrophoreticaly deposited CNTs electrode was examined using UV-VIS analysis as shown in Figure1. The absorbance Peak around 323 nm and 260 nm indicates the presence of Nickel nanostructures and optical properties of graphite respectively.

The composite electrode characterized by SEM as shown in figure 2. The Nickel (Ni) deposit on the CNTs electrode exhibits spherical shape having the size range 20 to 60 nm. This large size of Ni nanoparticles indicates agglomeration of Ni NPs of much finer size. As the size proliferate, some adjacent particles coalesce and some particles suffer diffusion interference due to their random distribution resulting in aggregation [29]. The SEM image of electrophoreticaly deposited CNTs electrode is also shown in Figure 2b. The Surface morphology clearly shows well dispersed CNTs.
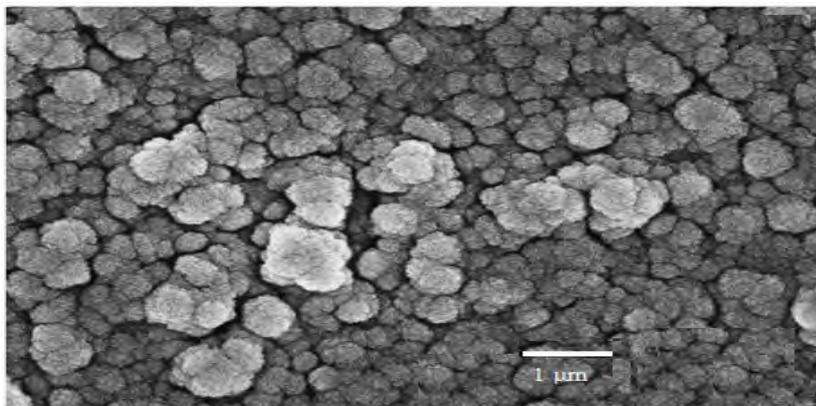

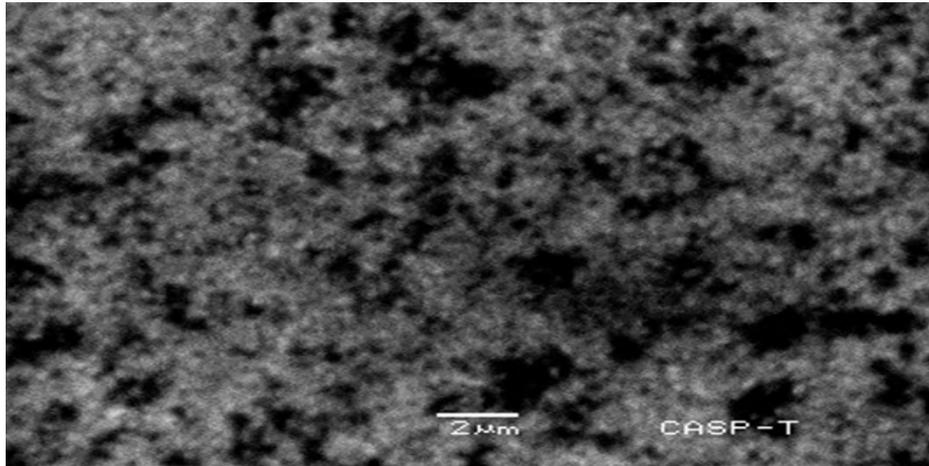Figure 2a: SEM image of Ni/CNTs/FTO nanocomposite electrode

Figure 2b: SEM image of CNTs/FTO modified electrode

The Ni/CNTs nanocomposite crystal structure was confirmed by using XRD determination (Figure 3). The X ray diffraction pattern indicates three peaks at 49.43, 55.23, and 76.42, corresponding to the planes {111}, {200}, and {220}, respectively, corresponds to the FCC Ni lattice. The peak at 33.05 is assigned to the [002] plane of the CNTs [30]. These results clearly show that the Ni nanoparticles have been successfully electrodeposited on the CNTs modified electrodes. Based on the experimental results and Scherrer formula, the average crystallite size of Ni was calculated to be 8 nm.
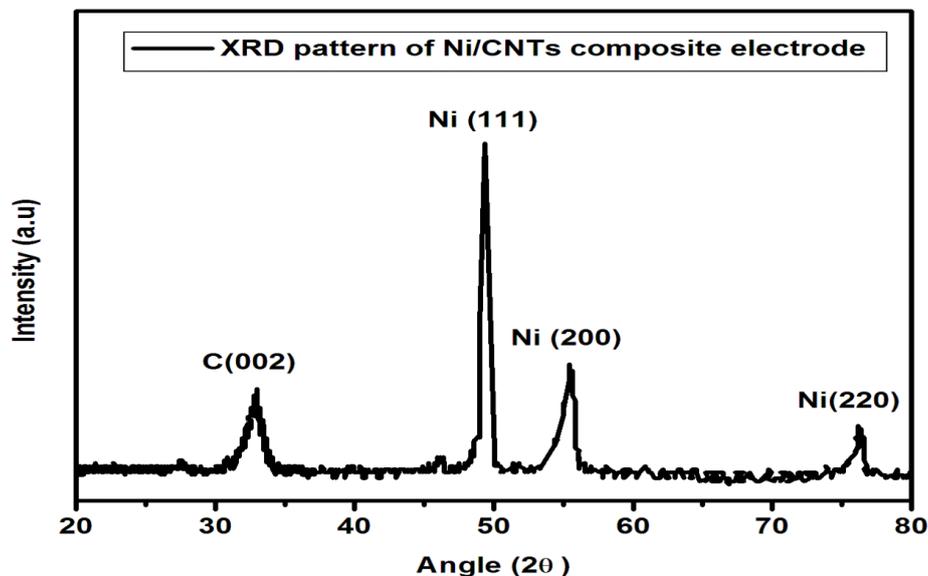

Figure 3: X-ray diffraction Pattern of Ni/CNTs/FTO nanocomposite Electrode

Therefore, the Ni nanoparticles of size 20-60 nm, perceived from the SEM images were assembled by the average Ni Nanocrystalline size of 8 nm. The growth of Ni nanoparticles on CNTs modified substrates provides Ni/CNTs nanocomposites having porous structure. Thus providing a perfect interface for utilizing in nonenzymatic electrochemical biosensor.

3.2 Electrochemical Characterization of Ni/CNTs/FTO electrode.

Figure 4 shows the comparison of Cyclic voltammograms of CNTs modified FTO substrate with Ni/CNTs modified FTO in 0.5 mM $K_3Fe(CN)_6$ and 0.1 M KCl at 50 mV/s. The reversible one electron redox behavior of Ferricyanide was observed. The voltammetric behavior of Ferricyanide redox couple on the CNTs electrode found due to the high aspect ratio and surface with electrocatalytic activity. For the Ni/CNTs nanocomposite electrode, the cyclic voltammetric response was comparable to that of the CNTs electrode. The voltammograms showed that Ni was efficiently immobilized on CNTs coated FTO surface providing the essential conduction paths to promote the transfer of electron at the interface of electrode and analyte like an electrode at nanoscale. With the Ni nanoparticles deposition on CNTs modified electrode, Peak current I_p has been increased and Peak separation (ΔE_p) decreased as compared to the CNTs modified electrode. This indicates that the Ni nanoclusters have increased the electrocatalytic active surface area.

The active surface area was calculated from the Randles–Sevcik equation ($I_p = 2.69{\times}10^5\ n^{3/2}\ ACv^{1/2}D^{1/2}$), where I_p is the Redox peak current (A), *n* is the electron transfer number (= 1), *A* is the surface area of the electrode (cm^2), *D* is the diffusion coefficient ($0.76 \times 10^{-5}\ cm^2/s$), *C* is the concentration of electroactive species ($K_3Fe(CN)_6$, M/L), and *v* is the scan rate (V/s). The calculated active surface areas of CNTs modified FTO and Ni/CNTs/FTO was 0.75 and 1.60 cm^2. These results clearly showed the increased active surface area of Ni/CNTs nanocomposite electrode.

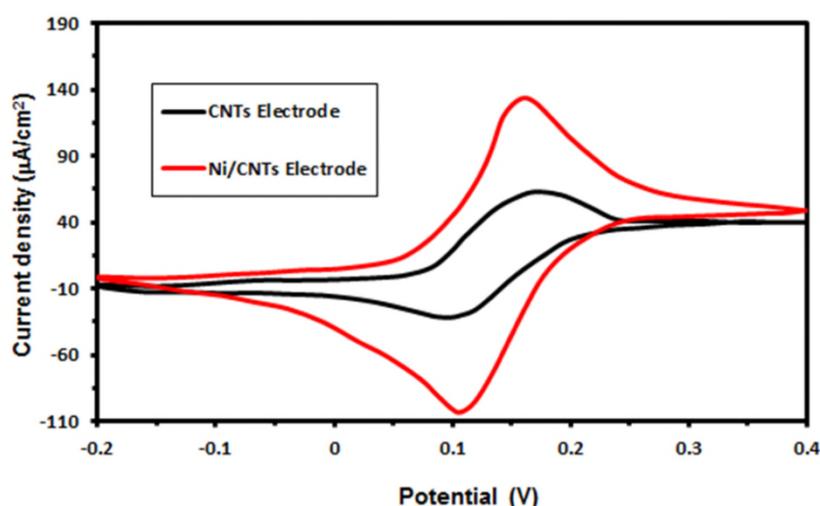*3.3 Non enzymatic Electrocatalysis of glucose at the Ni/CNTs/FTO electrode.*

Figure 4: Cyclic Voltammetry Curves of CNTs and Ni/CNTs/FTO electrode at scan rate of 50 mV/s

The electrocatalytic response of the CNTs/FTO and Ni/CNTs/FTO electrode towards glucose oxidation in alkaline media was examined by Cyclic voltammetry in 0.1 M NaOH solution at scan rate of 20 mV/s in the presence and absence of 0.5 mM glucose as shown in Figure 5. The potential range was selected from 0.0 to 0.8 V versus saturated calomel electrode (SCE). The requirement of alkaline medium to improve the effect of Ni for glucose oxidation is acknowledged. Figure shows that in the glucose absence, no Redox peaks appears from electrophoreticaly deposited CNTs electrode and Ni/CNTs composites electrode. A predominant increase in the reaction peak current was detected upon addition of glucose for Ni/CNTs composite as a working electrode. The well-defined pair of redox peak currents at 0.68 and 0.25 are observed from the voltammograms (d) corresponding to the glucose oxidation peaks for Ni (II)/Ni (III) [37-40]. Redox peaks from the transition of Ni (II) and Ni (III) have been considered as a mediator for electron transfer. These results indicate that Ni nanoparticles exhibit excellent electrocatalytic response towards glucose oxidation and CNTs electrode provides the large surface area and a high conductivity to increase the electron transfer rate. The detection potential was found 0.59 V.

Cyclic voltammetry plot of Ni/CNTs nanocomposite electrode in the presence of glucose (0.1 M NaOH) solution at altered scan rates 20 mV/s, 60 mV/s, 80 mV/s, 100 mV/s, and 150 mV/s is shown in Figure 6. The increasing scan rates resulted in shifting the redox peak currents to higher values with more peak to peak separation. Figure showed the linear variation of cathodic and anodic peak currents with increased square root of scan rates demonstrating that the electrochemical reactions are surface controlled by the adsorption of glucose molecule. The correlation coefficients R^2 0.985 and 0.989 for anodic and cathodic peaks, respectively have been observed.
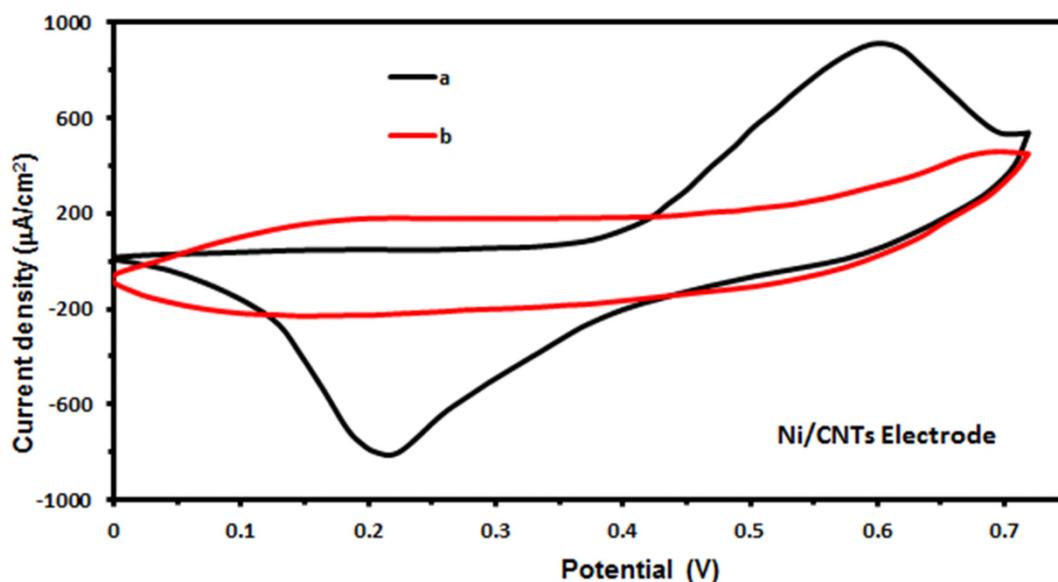

Figure 5: Cyclic Voltammetry of CNT electrode (Curves a and b) and Ni/CNT electrode (curves c and d) before (curves a and c) and after (Curves b and d) adding 0.5mM glucose in 0.1mM NaOH solution at scan rate of 20 mV/s
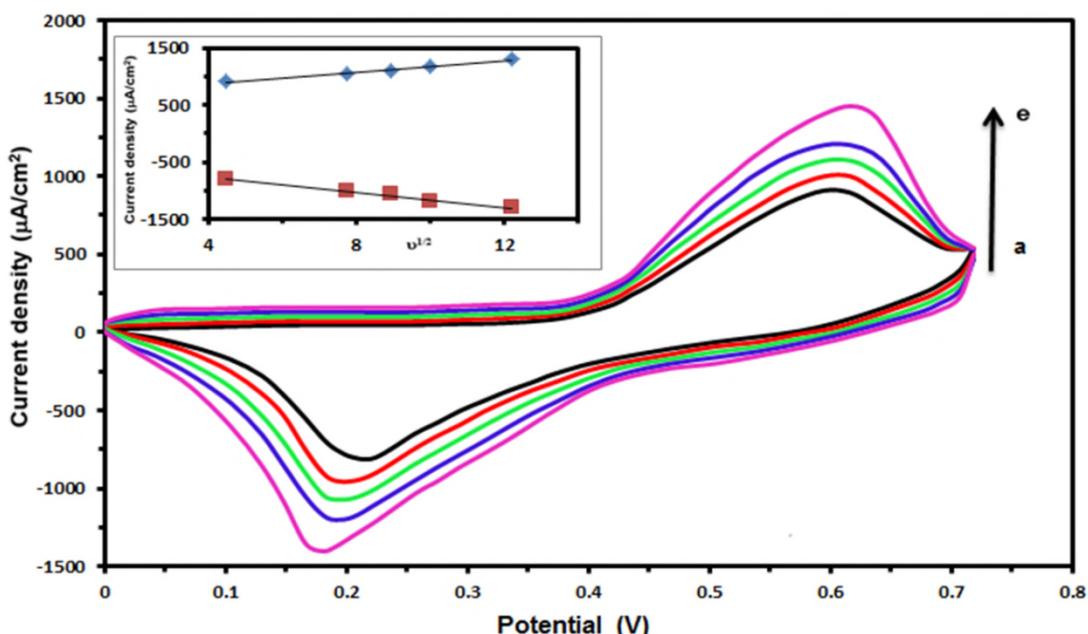
Figure 6: Cyclic Voltammetry Curves of Ni/CNTs/FTO electrode at various scan rates

3.4 Glucose detection response of Ni/CNTs/FTO electrode

Figure 7 demonstrate the amperometric results of Ni/CNTs composite electrode at optimized Potential (0.55V). The glucose by varying concentration was successively added in NaOH solution of optimized concentration 0.1 M. Each step of glucose addition generates a rise in current and gets a steady current in less than 4 s. This indicated an extremely rapid and subtle response of Ni/CNTs nanocomposite electrode toward glucose along with rapid diffusion of glucose.   The electrophoreticaly deposited CNTs electrode promoted fast transfer of electron providing high electro conductive performance.

The inset of Figure 7 showed the current density ($\mu A/cm^2$) vs. glucose concentration (mM) plot exhibiting linearity. The plot gives correlation coefficient R^2 0.992 and the sensitivity of Ni/CNTs nanocomposite sensor (605.0 μA mM^{-1} cm^{-2}). The limit of detection found 5.0 μM. This can be assigned to Ni nanostructures having high surface area and conductivity.

3.5 Stability and Reproducibility of the Ni/CNTs/FTO electrode

The reproducibility of the nonenzymatic glucose sensor was examined by making five Ni/CNTs nanocomposite electrodes with same fabrication technique and testing their current responses with 0.5 mM glucose solution in 0.1 M NaOH solution. After five successive measurements, the reproducible generated current was evaluated having relative standard deviation (RSD) of 4.2%. The RSD of successive 5 electrodes gives RSD of 5.2%. These results show the high reproducibility of Ni/CNTs electrode for glucose detection. The stability evaluation of electrode was performed by evaluating the current response to 0.5 mM glucose, each with 2 days intervals, as shown in Figure 8. The Ni/CNTs electrode was placed in air, when it was not measured. It was detected

that the current response could persist about 90% of its first value after storing for 23 days, revealing that the electrode offers very good stability.
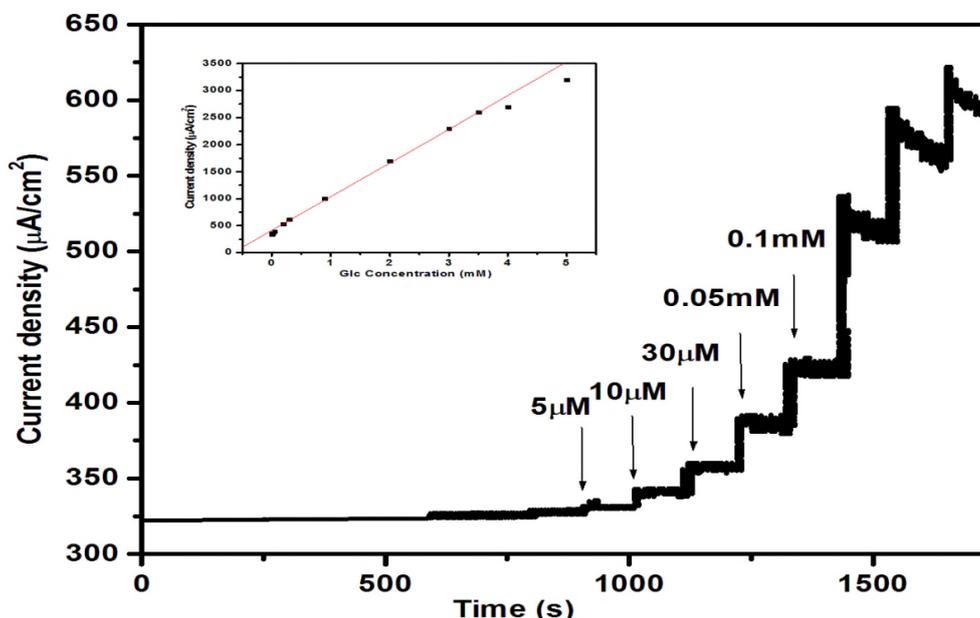

Figure 7: Current time response of Ni/CNTs/FTO electrode to various concentration of glucose in 0.1M NaOH solution. Inset: Current response versus glucose concentration.
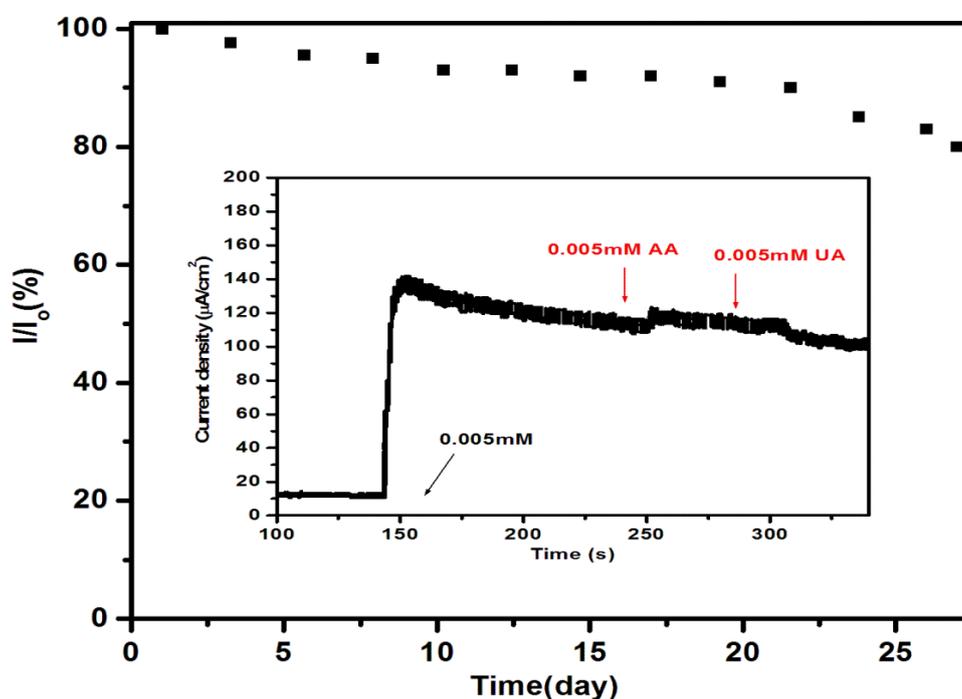

Figure 8: Stability of the Ni/CNTs/FTO electrode. The determination solution is 0.1M NaOH with 0.5mM glucose at 0.65V.Inset: Interference test of Ni/CNTs electrode with 0.005mM glucose and 0.005 mM each ascorbic acid (AA) and Uric acid (UA)

Some easily oxidized synergetic compounds such as ascorbic acid (AA) and uric acid (UA) gives interfering current signals which are the major encounters in the nonenzymatic detection of glucose. Although these intrusive species of AA (0.002 mM) and UA (0.002 mM) are much lower in concentration than glucose (3– 8 mM) in an ordinary biological sample, they generate electrochemical current values analogous to glucose. This might be due to more transfer of electrons [13]. The Inset of Figure 8 demonstrated the measurements upon addition of 0.005 mM interfering species with continuous addition of glucose in 0.1 M NaOH solution. A significant glucose response was detected as compared to glucose thereby neglecting the effect of interfering species. This demonstrates that the fabricated Ni/CNTs nanocomposite electrode is precisely specific towards glucose regardless of the intrusive species.

This work provides high sensitivity, fast response, low detection limit and good stability as compared to previously reported works [31-36]. In Comparison to other Ni/CNTs nanocomposite electrodes, the demonstrated advantages of the Ni deposition on the uniform and homogeneous CNT films showed that these CNT films played highly important role in glucose electrocatalytic oxidation performance. The improved performance can also be attributed to synergistic electrocatalytic behavior of the CNT films towards glucose oxidation [31]. This work offers a simple and a promising approach to functionalize the CNT thin films for possible application.

Conclusion

The Ni nanoparticles have been electrodeposited by Cyclic Voltammetry on the CNTs film prepared on FTO substrate by electrophoretic deposition, constructing a non-enzymatic amperometric glucose biosensor. The prepared Ni/CNTs/FTO electrode exhibits fast response of less than 4 s, high stability, good reproducibility and excellent sensitivity 605.0 $\mu A\ mM^{-1}\ cm^{-2}$ with wide linear range (0.005–3.5 mM) and low detection limit (5 μM). This value of sensitivity is higher in comparison to previously reported Ni electrodeposited nonenzymatic glucose sensors, demonstrating the increase in electrocatalytic active surface area by homogenous deposition of Ni nanoparticles on uniformly coated CNTs substrate. The glassy carbon electrode can be replaced with inexpensive FTO substrate for effective glucose determination with low detection limit, low over potential and high sensitivity. This project offers a promising approach to incorporate the CNTs thin films, prepared by Electrophoretic deposition, for potential application. Furthermore nanocomposites Ni/Cu/CNT are in process of fabrication by same technique for more sensitive nonenzymatic glucose detection.

References

Ricard Prehn , Montserrat Cortina-Puig and Francesc Xavier Munoz, *Journal of The Electrochemical Society*. **159** (2012) F134-F139.

Feihong Menga,Wei Shia, Yanan Suna, Xuan Zhub, Guisen Wua, Changqing Ruana, Xin Liua, Dongtao Gea, *Biosensors and Bioelectronics*.**42** (2013) 141-147.

Bansi D. Malhotraa, Asha Chaubeyb, S.P. Singha, *Analytica Chimica Acta*, **578** (2006) 59-74.

Joseph Wang,*Chemical Reviews*.**108** (2008) 814-825.

Sejin Park, Sun Young Lee,Hankil Boo, Hyun-Mi Kim,Ki-Bum Kim, et al, *Chemistry in Materials*.**19**(2007) 3373-3375.

Yipeng Sun, Harvey Buck, and Thomas E. Mallouk, *Analytical Chemistry*. **73** (2001) 1599-1604.

Hongtao Zhao, Huangxian Ju, *Analytical Biochemistry*. **350** (2006) 138–144   .

Arben Merkoc¸ Martin Pumera, Xavier Lopis, Briza Perez, Manel del Valle, Salvador Alegret, *Trends in Analytical Chemistry*. **24** (2005)   9.

Vasilis G. Gavalasa, Stacy A. Lawa, J. Christopher Balla, Rodney Andrewsb, Leonidas G. Bachasa, *Analytical Biochemistry*.**329** (2004)247-252.

Yuehe Lin , Xiaoli Cui1, Xiangrong Ye, *Electrochemistry communications*.**7** (2005) 267-274.

M.L. Mena, P. YanezSedeno, J.M. Pingarron, *Analytical Biochemistry*.**336** (2005)20-27.

Christine M. Welch, Richard G. Compton, *Analytical and Bioanalytical Chemistry*.**384** (2006) 601-619.

Sejin Park, Taek Dong Chung and Hee Chan Kim, *Analytical Chemistry*. **75** (2003) 3046-3049.

Hankil Boo, Sejin Park, Bonkyung Ku,Yunmee Kim, Jin Hyung Park, Hee Chan Kim and Taek Dong Chung, *American Chemical Society*.**126** (2004) 4524-4525.

Innocenzo G Casella , Maria Gatta, Maria R Guascito, Tommaso R.I Cataldi, *Analytica Chimica Acta*. **357** (1997) 63-71.

Qin Xu, Yu Zhao, Jin Zhong Xu, Jun-Jie Zhu, *Sensors and Actuators B*. **8694** (2005)1-8.

Masato Tominaga, Toshihiro Shimazoe, Makoto Nagashima, Isao Taniguchi, *Electrochemistry communications*.**7** (2005) 189-193.

Masato Tominaga, Toshihiro Shimazoe, Makoto Nagashima, Hideaki Kusuda,
Atsushi Kubo, Yutaka Kuwahara and Isao Taniguchi, *Electroanalytical Chemistry*.**590** (2006) 37-46.

Tianyan You ,Osamu Niwa , Zilin Chen , Katsuyoshi Hayashi , Masato Tomita and Shigeru Hirono , *Analytical chemistry*. **75**(2003) 5191-5196.

JianShan Yea, Ying Wenb, Wei De Zhangc, Leong Ming Ganc, Guo Qin Xub, FwuShan Sheua,, *Electrochemistry communications*. **6** (2004) 66-70.

Randhir P. Deo, Joseph Wang, *Electrochemistry communications*. **6** (2004) 284-287.

Keith B Malea, Sabahudin Hrapovica, Yali Liua, Dashan Wangb, John H.T Luonga, *Analytica Chimica Acta*.**516**   (2004) 35-41.

Joseph Wang, Gang Chen, Mei Wang and Madhu Prakash Chatrathia, *Analyst*.**129** (2004)512-515.

Shamsipur, Mojtaba, Mostafa Najafi, and Mohammad-Reza Milani Hosseini, B*ioelectrochemistry* **77.2** (2010): 120-124.

Yanhui Xu, Xiangqin Lin, *Electrochimica Acta*. **52** (2007) 5140-5149.

Laxmidhar Besra, Meilin Liu, *Progress in Materials Science*. **52** (2007)1–61.

I ZHITOMIRSKY, L GALOR,*Materials in Medicine*. **8** (1997)213-219.

I. Zhitomirsky, *J. European Ceramic Society*. **18** (1998)849–856.

Linyou Cao , Peng Diao , Tao Zhu and Zhongfan Liu , *J. Physical Chemistry B*.**108** (2004) 3535-3239.

M. Terrones, W.K. Hsu, A. Schilder, H. Terrones et al. , *Applied Physics A*. **66** (1998) 307-317.

Sun, Aili, Jianbin Zheng, and Qinglin Sheng. *Electrochimica Acta* **65** (2012): 64-69.

Bittencourt, C., et al. *Surface science* **601.13** (2007): 2800-2804.

Rather, Sami-ullah, and Kee Suk Nahm. *Materials Research Bulletin* **49** (2014): 525-530.

Hsieh, Chien-Te, Yun-Wen Chou, and Wei-Yu Chen. *Journal of Solid State Electrochemistry* **12.6** (2008): 663-669.

Zhu, Z. G., et al. *Sensors and Actuators B: Chemical* **178** (2013): 586-592.

Lin, Kuan-Yu, Wen-Ta Tsai, and Jeng-Kuei Chang. *International journal of hydrogen energy* **35.14** (2010): 7555-7562.

Lu, Li-Min, et al. *Biosensors and Bioelectronics* **25.1** (2009): 218-223.

Salimi, Abdollah, and Mahmoud Roushani. *Electrochemistry Communications* **7.9** (2005): 879-887.

Ai, Hanhua, et al. *Biosensors and Bioelectronics* **24.4** (2008): 1048-1052.

Wang, Yulong, et al. *Sensors and Actuators B: Chemical* **151.1** (2010): 65-70.